Eur. Phys. J. E (2009)
DOI 10.1140/epje/i2009-10485-7

THE EUROPEAN PHYSICAL JOURNAL E

Regular Article

The UV-vis absorption spectrum of the flavonol quercetin in methanolic solution: A theoretical investigation

T. Andrade-Filho[a], T.C.S. Ribeiro, and J. Del Nero[b]

Instituto de Física, Instituto de Ciências Exatas e Naturais, Universidade Federal do Pará, 66075-110, Belém, Pará, Brazil

Received 4 February 2009 and Received in final form 24 April 2009

Abstract. The UV-vis absorption spectrum of the solvated quercetin molecule in methanol was investigated theoretically by means of an elegant type of QM/MM scheme better known as sequential Monte Carlo/quantum mechanics (S-MC/QM) methodology. A set of 125 uncorrelated Monte Carlo molecular liquid structures were properly selected through the autocorrelation function of the energy in order to be used in the quantum mechanical calculations. These molecular liquid structures were obtained by means of the radial and minimum distance distribution functions. A detailed account of the pattern of hydrogen bond structures obtained in this study is also available. The computed results obtained here were directly compared with the available experimental data in order to validate our theoretical model and through this comparison a very good conformity between theoretical and available experimental results was found.

PACS. 61.20.Ja Computer simulation of liquid structure – 36.20.Kd Electronic structure and spectra – 31.70.Dk Environmental and solvent effects

1 Introduction

Flavonoids are polyphenolic compounds mainly found in grapes, wine, apples, tea and berries [1,2]. They have attracted considerable attention of the scientific community due to their biological and pharmacological properties, such as for example, antioxidant, anticarcinogenic, anti-inflammatory, antiviral and anti-allergic features [3–5]. Based on structure, flavonoids are divided into several classes such as catechins, anthocyanidins, isoflavones, flavones, flavanones and flavonols. Interest in the biological properties of flavonoids has increased over the years since the emergence of the French paradox phenomenon.

This phenomenon derived from the observation of low coronary heart disease death rates despite a high saturated fat diet [6–9]. According to some studies, the daily consumption of red wine by the French is one of the main factors behind this phenomenon [10]. This explanation is strongly supported by the high concentration of polyphenolic compounds, principally the flavonol quercetin, in the beverage under discussion [6].

The flavonol quercetin (3, 3′, 4′, 5, 7-pentahydroxyflavone) (QC) (see fig. 1), a phytoalexin, is one of the most potent biomedical agents known. Several types of diseases are inhibited by this biocompound such as cataract, coronary heart disease, diabetes and cancer, especially prostate cancer [11–16]. Together with the flavonol kaempferol, quercetin is one of the most abundant flavonoids in the human diet [17].

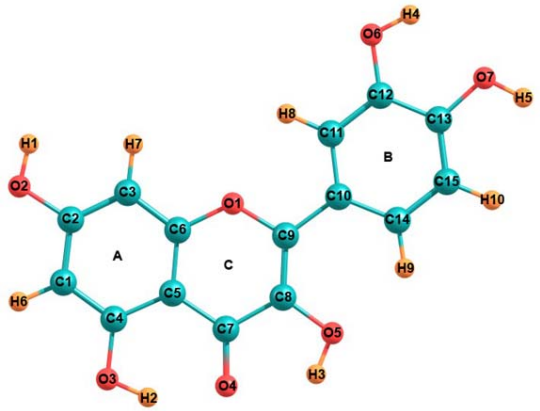

Fig. 1. (Color online) The structure of QC and its atomic indices used in table 1.

Regrettably, similar to the most important stilbene resveratrol and other biocompounds, the biological features of QC are not clearly understood [18]. Over the years, as an effort to understand unclear biological properties, molecular structural and electronic properties of organic compounds in gas phase have been analyzed and correlated to their inherent biological properties [19–23].

[a] e-mail: tarciso@ufpa.br
[b] e-mail: jordan@ufpa.br

Published online: 04 July 2009

Nevertheless, in nature, biocompounds are found in most liquid environments. For this reason, in the current theoretical investigation, in order to better understand the electronic properties of the flavonol under investigation in a realistic environment, we thus simulate the UV-vis absorption spectrum of quercetin in methanolic solution by means of the QM/MM scheme developed by Coutinho and Canuto better know as sequential Monte Carlo/quantum mechanical (S-MC/QM) methodology [24].

The inclusion of the methanol solvent molecules [25–27] in the UV-vis absorption spectrum QM calculations of the quercetin molecule was properly obtained by means of the radial and minimum distance distribution functions. The structures connected via hydrogen bonds were also investigated.

The aim of this molecular liquid simulation is to study how the $\pi \rightarrow \pi^*$ transition energy of QC is modified through the discrete process of inclusion of methanol molecules within the hydrogen bond, micro, first and second solvation shells for use in performing QM calculations [26–28].

The theoretical model proposed here was directly compared with the available experimental observations in order to be validated and through this comparison a very good agreement between theoretical and available experimental results was found.

2 Computational details

Our calculations started with the geometry optimization of quercetin in vacuum by means of the Gaussian 98 suite of programs [29]. It was treated quantum mechanically by the well-established hybrid B3LYP density functional and 6-31+G(d) basis set. Our molecular liquid simulation was performed in a cubic cell with a total of 1000 OPLS-UA [30] methanol solvent molecules and a QC molecule as solute.

The non-electrostatic Lennard-Jones parameters of QC molecule were obtained from the OPLS-AA force field (see table 1) [31]. The partial charges of QC were computed via Breneman-Wiberg CHELPG fitting scheme [32] using the B3LYP/6-31+G(d) level of computation. The Metropolis MC simulation was carried out by DICE program [33].

Metropolis MC algorithm and periodic boundary conditions under the minimum image convention technique [34] were used in the canonical (NVT) ensemble. The simulation cell with dimensions $40.870 \times 40.870 \times 40.870\,\text{Å}^3$ was determined by the density of liquid methanol ($0.7866\,\text{g/cm}^3$) at room temperature [35]. The intermolecular non-bonded interactions were calculated through the sum of Lennard-Jones and Coulomb potential functions.

A non-bonded spherical cutoff radius of 20.435 Å was used to truncate the intermolecular non-bonded interactions [34]. The molecular liquid was thermalized for 5.0×10^7 MC steps followed by a production stage of 2.0×10^8 MC steps. The molecular geometries of the solute and solvent molecules used here were kept rigid in the course of the thermalization and production stages.

Table 1. Lennard-Jones parameters, charge distribution and the computed gas phase dipole moment (in Debye) for QC molecule.

Site	ε (kcal/mol)	σ (Å)	q (a.u.)
C1	3.550	0.070	0.272
C2	3.550	0.070	0.396
C3	3.550	0.070	−0.384
C4	3.550	0.070	0.262
C5	3.550	0.070	0.662
C6	3.500	0.066	0.148
C7	3.500	0.066	−0.003
C8	3.550	0.070	0.148
C9	3.550	0.070	0.220
C10	3.500	0.066	−0.321
C11	3.550	0.070	0.467
C12	3.550	0.070	−0.525
C13	3.550	0.070	0.667
C14	3.550	0.070	−0.570
C15	3.550	0.070	0.623
O1	2.900	0.140	−0.172
O2	3.070	0.170	−0.658
O3	3.070	0.170	−0.661
O4	2.960	0.210	−0.550
O5	3.070	0.170	−0.628
O6	3.070	0.170	−0.714
O7	3.070	0.170	−0.699
H1	0.000	0.000	0.455
H2	0.000	0.000	0.499
H3	0.000	0.000	0.435
H4	0.000	0.000	0.462
H5	0.000	0.000	0.463
H6	2.420	0.030	0.245
H7	2.420	0.030	0.193
H8	2.420	0.030	0.217
H9	2.420	0.030	0.144
H10	2.420	0.030	0.142
Dipole moment		$\mu = 5.37\,\text{D}$	

In order to generate a new configuration, one needs to randomly translate along the three Cartesian coordinate directions all the methanol solvent molecules and rotate them about a randomly chosen axis by $\delta\theta = \pm 15°$. Therefore, new configurations are produced after 1.0×10^3 MC steps.

In fact, by means of the S-MC/QM procedure, one can compute the UV-vis absorption spectrum of a solvated molecule through a series of QM calculations on the molecular liquid structures produced by the MC simulation [24,28]. Solely, the hydrogen bond, micro, first and second solvation shells were treated by the QM In-

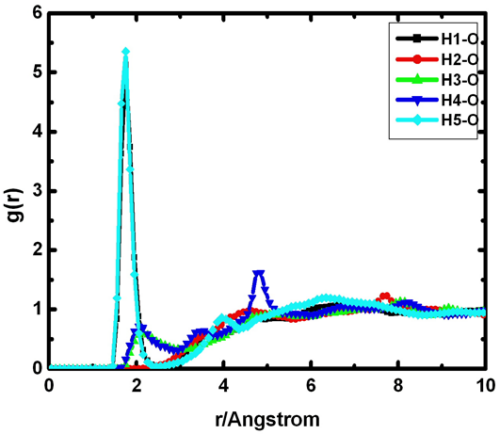

Fig. 2. (Color online) Radial pair distribution functions between the hydroxyl hydrogens of QC and methanol hydroxyl oxygen.

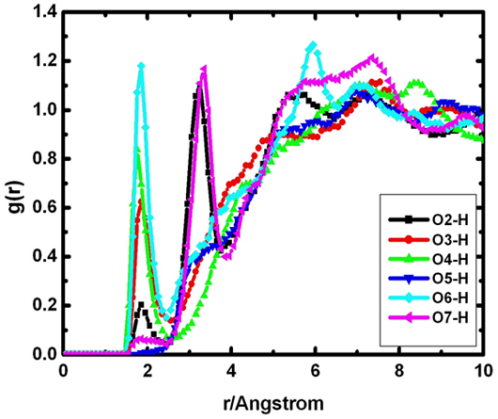

Fig. 3. (Color online) Radial pair distribution functions between the hydroxyl and carbonyl oxygens of QC and methanol hydroxyl hydrogen.

termediate Neglect of Differential Overlap/Spectroscopic-Configuration Interaction (INDO/S-CI) scheme.

In this combined technique, to compute the average value of the $\pi \rightarrow \pi^*$ transition energy of the quercetin we sampled and averaged each single value gathered from the MC liquid configurations [27,28]. In fact, all these selected configurations are considered statistically relevant [27,28]. The refined form that these functions are obtained as well as the technique of selecting uncorrelated configurations is described in details in refs. [26–28].

Through this technique, 125 uncorrelated configurations with less than 15% of statistical correlation were selected [26–28]. In fact, the average values of the $\pi \rightarrow \pi^*$ transition energies were safely computed as a simple average of the values produced by each uncorrelated configuration because the Boltzmann function was considered in the Metropolis MC importance sample algorithm [28]. The UV-vis absorption spectrum was computed by the INDO/S-CI scheme [36] implemented in the ZINDO package [37].

3 Results and discussion

3.1 Hydrogen bond structures

In general, the mechanisms responsible for the antioxidant features of polyphenolic compounds are governed by the donation of hydroxyl hydrogens to free radicals [38]. This is possible due (mainly) to the number and localization of hydroxyl groups of these compounds [39] as well as hydrogen bonds [38]. The role played by the hydrogen bonds (HBs) is to repair the damage suffered in the structure of these biocompounds when they donate hydroxyl hydrogens to free radicals [38]. It is of crucial importance for human health because it can prevent the formation of new and perhaps more potent free radicals [38].

Since the functioning of biomolecules is profoundly affected by the solvent medium around them [40], at this time we will study the formation of HBs between the solute and the solvent molecules under investigation. An average picture of the HB methanol molecules around the QC can be provided by means of the radial distribution functions [41]. Figure 2 depicts the radial distribution functions associated with the quercetin hydroxyl hydrogens and methanol oxygen ($g_{\text{H-O}}$). In fig. 3 we show the radial distribution functions associated with the quercetin hydroxyl and carbonyl oxygens and methanol hydroxyl hydrogen ($g_{\text{O-H}}$). The $g_{\text{H-O}}$ radial distribution functions ($g_{\text{H1-O}}$, $g_{\text{H2-O}}$, $g_{\text{H3-O}}$, $g_{\text{H4-O}}$ and $g_{\text{H5-O}}$) start at 1.42, 2.19, 1.63, 1.58 and 1.42 Å and present a first peak maximum located at 1.76, 2.33, 2.17, 2.04 and 1.77 Å, respectively [27,28]. The respective spherical integration performed up to the first minimum of the $g_{\text{H1-O}}$, $g_{\text{H2-O}}$, $g_{\text{H3-O}}$, $g_{\text{H4-O}}$ and $g_{\text{H5-O}}$ radial distribution functions at 2.55, 2.53, 3.02, 2.92 and 2.46 Å yields a coordination number of 1.00, 0.01, 0.61, 0.58 and 0.99.

The $g_{\text{O-H}}$ radial distribution functions ($g_{\text{O2-H}}$, $g_{\text{O3-H}}$, $g_{\text{O4-H}}$, $g_{\text{O5-H}}$, $g_{\text{O6-H}}$ and $g_{\text{O7-H}}$) start at 1.51, 1.45, 1.42, 1.46, 1.47 and 1.52 Å and have a first peak maximum at 1.82, 1.80, 1.78, 1.85, 1.75 and 1.79 Å [27,28]. An amount of 0.07, 0.24, 0.24, 0.01, 0.35 and 0.38 nearest neighbors were found through the integration performed in the $g_{\text{O2-H}}$, $g_{\text{O3-H}}$, $g_{\text{O4-H}}$, $g_{\text{O5-H}}$, $g_{\text{O6-H}}$ and $g_{\text{O7-H}}$ radial distribution functions up to their respective first minimum at 2.45, 2.59, 2.55, 2.08, 2.46 and 2.49 Å.

The technique used here to detect structures linked by hydrogen bonds was based in a combination of geometric and energetic criteria. This combination has been successfully applied before by Coutinho and Canuto in order to select the structures involved in HBs in liquids [27,28,42]. It is worth noting that in this simulation we selected the structures linked by hydrogen bonds according to a common criterion for each parameter to be described soon for each hydrogen bond site as applied before by Jedlovszky and Turi [43].

Quercetin and methanol molecules are linked by hydrogen bonds only if the three conditions, obtained in this simulation, are all together fulfilled: first, the RDA

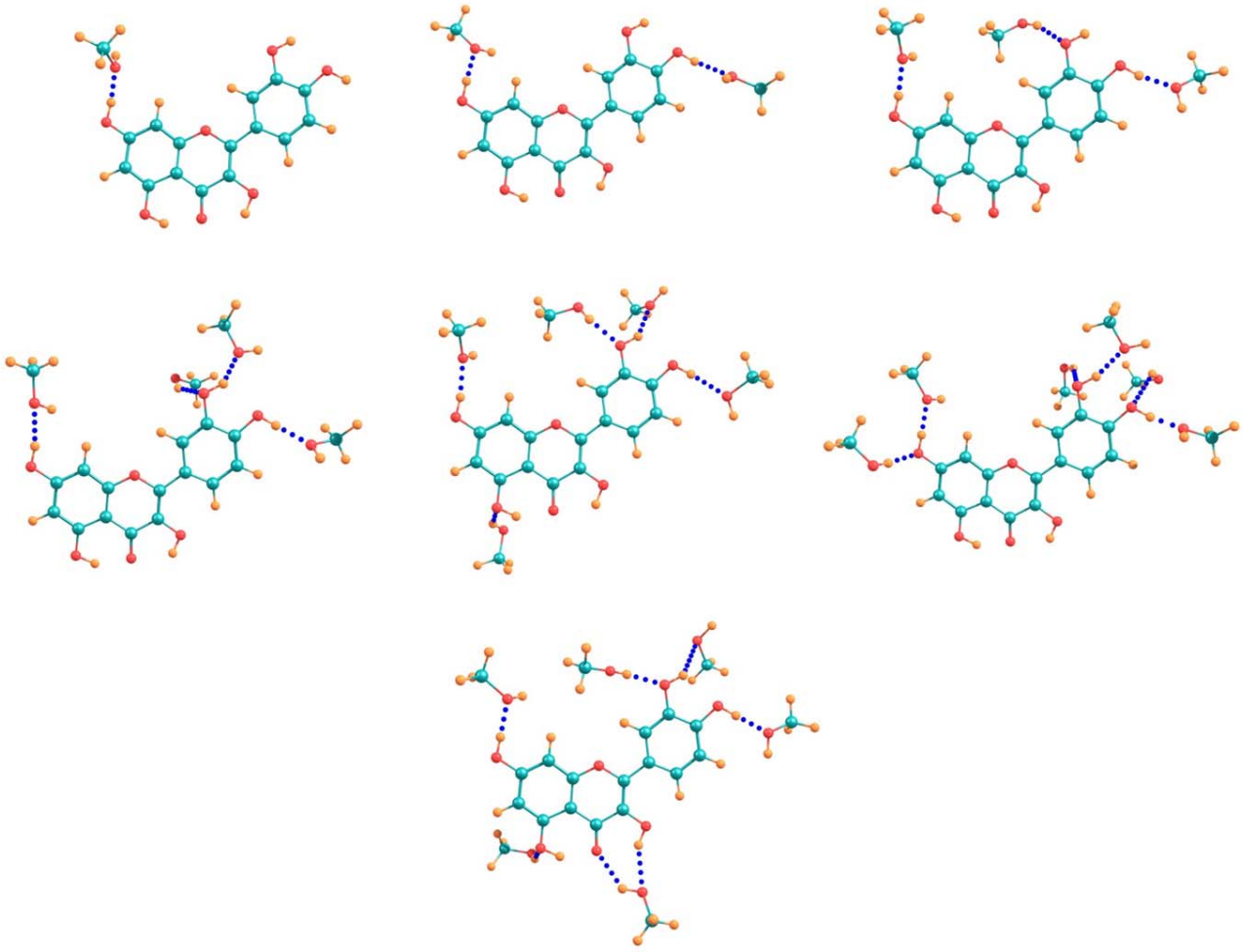

Fig. 4. (Color online) Snapshots of the hydrogen bond interactions between QC and methanol molecules.

Table 2. Statistics of the hydrogen bonds formed between QC and methanol and their $\pi \rightarrow \pi^*$ average transition energies.

Number of HBs	Occurrence (%)	$\pi \rightarrow \pi^*$ (nm)
1	0.4	358.4 ± 0.97
2	12.5	358.5 ± 1.13
3	23.5	356.3 ± 1.58
4	26.9	356.7 ± 0.89
5	23.5	358.5 ± 0.94
6	6.7	357.1 ± 1.03
7	6.5	357.2 ± 1.08
Total (HB shell)	100	357.4 ± 1.53

distance is closer than 3.5 Å. Second, the AHD angle is closer than 40° and third, the binding energy is larger than 6.0 kcal/mol [27,28,42,44,45].

In this sense, according to the set of three conditions considered in this study, a total amount of 446 HBs between QC and methanol solvent molecules were formed whose pattern of formation ranges from one to seven HBs (see fig. 4). The statistical data concerning the occurrence of the HBs formed in this work is outlined in table 2. As can be noticed, the majority of the uncorrelated configurations are involved in one to four hydrogen bonds (63.3%) [46].

It is apparent that the results reported above do not provide any information concerning the HB donor and acceptor ability of QC is available. We found that in 2.2, 6.2, 6.2, 0.4, 9.6 and 0.9% of the configurations, the O2, O3, O4, O5, O6 and O7 atomic sites act as acceptors of hydrogen bonds. In 26.4, 8.5, 11.4 and 28.2% of the configurations O2-H1, O5-H3, O6-H4, and O7-H5 groups act as donors of hydrogen bonds, respectively.

It was found that the O3-H2 group does not act as a donor of hydrogen bonds. From these results, it can be noticed that the O6 atomic site demonstrates the greatest ability to accept HBs and the O7-H5 group to donate HBs. Taking into account the antioxidant capacity, one can note through these results that the B-ring of quercetin (see fig. 1) is the more important site involved in donation of HBs compared to the A- and C-rings [47]. In fact, this is in agreement with the reported literature [47].

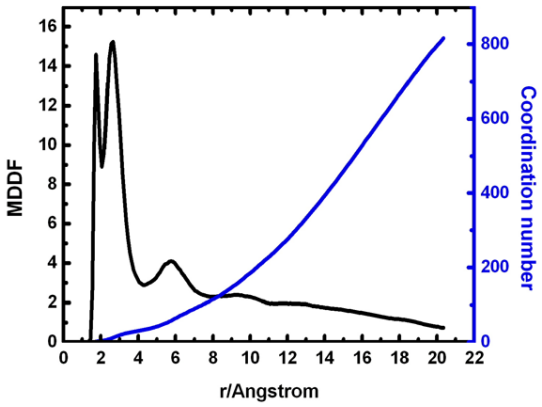

Fig. 5. (Color online) Minimum distance distribution function (MDDF) between the smallest distance of all QC atoms and all methanol atoms. The blue bold line corresponds to the coordination number obtained in the MDDF.

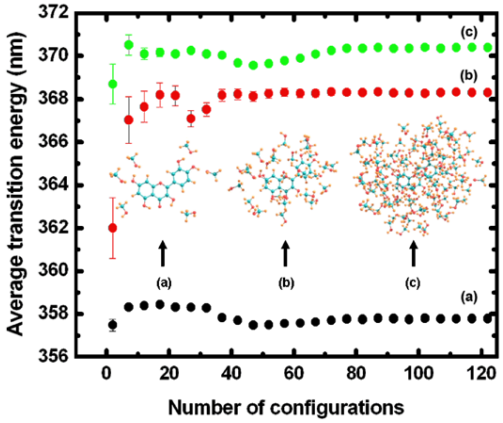

Fig. 6. (Color online) Statistical convergence of the average value of the $\pi \rightarrow \pi^*$ transition energy of QC in methanol obtained for the (a) micro, (b) first and (c) second solvation shells. A randomly chosen configuration of the micro (a), first (b) and second (c) solvation shells is also shown in this figure.

3.2 UV-vis spectrum

The gas phase absorption spectrum will be used as a starting point for the investigation of how the solvation changes the $\pi \rightarrow \pi^*$ transition energy of quercetin. After that, the solvation change under consideration is investigated through the results computed from the in-solution absorption spectrum. For the isolated case of the $\pi \rightarrow \pi^*$ transition energy a value of 352.7 nm was found. As far as we know, regrettably, this transition energy has not been reported experimentally to date. The in-solution absorption spectrum was computed in different forms using first, in the quantum mechanical calculations, the solvation provided by the methanol solvent molecules involved in HBs and then the micro, first and second solvation shells of methanol solvent molecules.

In order to start our discussions concerning the $\pi \rightarrow \pi^*$ transition energy of quercetin solvated in methanol, we outlined in table 2 the computed results of the referred transition energy of the QC solvated by hydrogen-bonded methanol molecules. From one to seven hydrogen bonds, the average value of the $\pi \rightarrow \pi^*$ transition energy was computed to be 358.4 ± 0.97, 358.5 ± 1.13, 356.3 ± 1.58, 357.7 ± 0.89, 358.5 ± 0.94, 357.1 ± 1.03 and 357.2 ± 1.08 nm, respectively. For the hydrogen bond shell as a whole, the average value of the $\pi \rightarrow \pi^*$ transition energy was computed to be 357.4 ± 1.53 nm. This computed value is not in good conformity when compared with the experimental observations of Robards *et al.* of 371 nm [48] and of Cornard *et al.* of 372 nm [49].

In order to have better comparison between theoretical and experimental results, we solvated the quercetin molecule with more solvent molecules by means of the first and second solvation shells and not only with the hydrogen-bonded methanol molecules. For comparative purposes with the HB shell, the micro solvation shell was also taken into account in the QM calculations.

Each one of the previously mentioned liquid structures of methanol molecules around of quercetin was obtained in the minimum distance distribution function (MDDF) (fig. 5) [50]. Taking into account the micro, first and second solvation shell liquid structures, the MDDF displays three minima located at 2.10, 4.21 and 7.69 Å, respectively. Coordination numbers of 6, 36 and 108 methanol molecules around the quercetin are computed through these respective minima.

For illustrative purposes, we have plotted in fig. 6 the average value of the $\pi \rightarrow \pi^*$ transition energy of the micro, first and second solvation shells. It was found that the average value of the $\pi \rightarrow \pi^*$ transition energy of the micro, first and second solvation shells converges at 357.7 ± 1.15, 368.3 ± 1.97 and 370.3 ± 2.11 nm, respectively.

These theoretical predictions are in rather better agreement with the experimental observations of 371 and 372 nm [48,49] than that computed for the hydrogen bond shell. The average computed value of the $\pi \rightarrow \pi^*$ transition energy obtained from micro solvation shell is only 0.38 nm larger than that one computed for the HB shell. Not necessarily hydrogen bonded to the QC molecule, the spectroscopy effect of methanol molecules of the micro solvation shell on the $\pi \rightarrow \pi^*$ transition energy of the QC is almost the same.

For our best result, the computed average value of the $\pi \rightarrow \pi^*$ transition energy obtained from the second solvation shell is 0.39 nm larger than the experimental observation of Robards *et al.* [48] and 0.61 nm lower than the experimental observation of Cornard *et al.* [49]. Also, it is worth noticing that our best average computed value for the $\pi \rightarrow \pi^*$ transition energy is in better agreement with the available experimental results of 371 and 372 nm than that one computed by Cornard *et al.* of 381 nm [49].

In fact, even using a few number of QM calculations, a fast convergence is attained as one can observe in fig. 6 [27,28]. This is thus attained due to the fact that we only sampled the configurations which are considered statistically relevant as discussed previously in several articles [27,28,51–53].

For a lack of experimental information we cannot compare the bathochromic shifts of the $\pi \rightarrow \pi^*$ calculated in the current work. However, as can be noticed, the solvation process simulated here indeed reproduced the available experimental results of the $\pi \rightarrow \pi^*$ transition energy of QC in methanolic solution [48,49].

4 Conclusion remarks

The sequential Monte Carlo/quantum mechanics technique was used here in order to compute the UV-vis absorption spectrum of the QC molecule solvated in methanol.

The structure of the molecular liquid was taken into account in this theoretical investigation by means of the minimum distance and radial distribution functions. The main feature of the HB ability of QC is the greatest capacity to donate HBs at the O7-H5 group as well as accept HBs at the O6 atomic site.

The QM calculations were based on the semiempirical INDO/S-CI methodology in the uncorrelated configurations selected from the MC simulation. The average $\pi \rightarrow \pi^*$ transition energy obtained from the second solvation shell, our best result, is in very good agreement to the available experimental results of 371 and 372 nm.

Finally, as can be clearly noticed, the model proposed here for the $\pi \rightarrow \pi^*$ transition energy matches very well with the available experimental results.

We would like to acknowledge Prof. S. Canuto and Prof. K. Coutinho for providing their high level Monte Carlo simulation program DICE. This work was supported by the Brazilian agencies PIBIC/CNPq, CNPq and FAPESPA.

References

1. J. Duarte, R. Pérez-Palencia, F. Vargas, M.A. Ocete, F. Pérez-Vizcaino, A. Zarzuelo, J. Tamargo, Brit. J. Pharmac. **133**, 117 (2001).
2. S. Fiorucci, J. Golebiowski, D. Cabrol-Bass, S. Antonczak, Chem. Phys. Chem. **5**, 1726 (2004).
3. Y.K. Rao, S. Fang, Y. Tzeng, J. Ethnopharmacol. **100**, 249 (2005).
4. D. Xie, S.B. Sharma, N.L. Paiva, D. Ferreira, R.A. Dixon, Science **229**, 396 (2003).
5. D.J. Bauer, J.W.T. Selway, J.F. Batchelor, M. Tisdale, I.C. Caldwell, D.A.B. Young, Nature **292**, 369 (1981).
6. J.V. Formica, W. Regelson, Food Chem. Toxicol. **33**, 1061 (1995).
7. E.N. Frankel, J. Kanner, J.B. German, E. Parks, J.E. Kinsella, Lancet **341**, 454 (1993).
8. S. Renaud, M. de Lorgeril, Lancet **339**, 1523 (1992).
9. M. Law, N. Wald., Br. Med. J. **318**, 1471 (1999).
10. J. Ferrières, Heart **90**, 107 (2004).
11. S.D. Varma, A. Mizuno, J.H. Kinoshita, Science **195**, 205 (1977).
12. Y.J. Zhang, N.P. Seeram, R. Lee, L. Feng, D. Heber, J. Agric. Food Chem. **56**, 670 (2008).
13. S.D. Varma, I. Mikuni, J.H. Kinoshita, Science **188**, 1215 (1975).
14. N. Mahmood, S. Piacente, C. Pizza, A. Burke, A.I. Khan, A.J. Hay, Biochem. Biophys. Res. Com. **229**, 73 (1996).
15. S.R. Muir, G.J. Collins, S. Robinson, S. Hughes, A. Bovy, C.H. Ric De Vos, A.J. van Tunen, M.E. Verhoeyen, Nature Biotech. **19**, 470 (2001).
16. Y. Zhang, A.Y. Chen, M. Li, C. Chen, Q. Yao, J. Surg. Res. **148**, 17 (2008).
17. C. Manach, C. Moranda, V. Crespy, C. Demigné, O. Texier, F. Régérat, C. Rémésy, FEBS Lett. **426**, 331 (1998).
18. A.R. Parker, V.L. Welch, D. Driver, N. Martini, Nature **426**, 786 (2003).
19. C.L. Ham, P.C. Jurs, Chem. Sens. **10**, 491 (1985).
20. F. Gasparrini, I. D'Acquarica, M. Pierini, C. Villani, J. Separ. Sci. **24**, 941 (2001).
21. F.J.B. Cardoso, A.F. de Figueiredo, M.D.S. Lobato, R.M. de Miranda, R.C.O. de Almeida, J.C. Pinheiro, J. Mol. Model. **14**, 39 (2008).
22. L.E. Korhonen, M. Turpeinen, M. Rahnasto, C. Wittekindt, A. Poso, O. Pelkonen, H. Raunio, R.O. Juvonen, Brit. J. Pharmacol. **150**, 932 (2007).
23. S. Mukherjee, A. Mukherjee, A. Saha, J. Mol. Struc. (Theochem.) **715**, 85 (2005).
24. K. Coutinho, S. Canuto, Adv. Quantum Chem. **28**, 89 (1997).
25. H. Lin, D.G. Truhlar, Theor. Chem. Acc. **117**, 185 (2007).
26. H.C. Georg, K. Coutinho, S. Canuto, J. Chem. Phys. **123**, 124307 (2005).
27. W.R. Rocha, V.M. Martins, K. Coutinho, S. Canuto, Theor. Chem. Acc. **108**, 31 (2002).
28. K. Coutinho, S. Canuto, J. Mol. Struct. (Theochem.) **632**, 235 (2003).
29. M.J. Frisch, G.W. Trucks, H.B. Schlegel, G.E. Scuseria, M.A. Robb, J.R. Cheeseman, V.G. Zakrzewski, J.A. Montgomery jr., R.E. Stratmann, J.C. Burant, S. Dapprich, J.M. Millam, A.D. Daniels, K.N. Kudin, M.C. Strain, O. Farkas, J. Tomasi, V. Barone, M. Cossi, R. Cammi, B. Mennucci, C. Pomelli, C. Adamo, S. Clifford, J. Ochterski, G.A. Petersson, P.Y. Ayala, Q. Cui, K. Morokuma, D.K. Malick, A.D. Rabuck, K. Raghavachari, J.B. Foresman, J. Cioslowski, J.V. Ortiz, A.G. Baboul, B.B. Stefanov, G. Liu, A. Liashenko, P. Piskorz, I. Komaromi, R. Gomperts, R.L. Martin, D.J. Fox, T. Keith, M.A. Al-Laham, C.Y. Peng, A. Nanayakkara, C. Gonzalez, M. Challacombe, P.M.W. Gill, B. Johnson, W. Chen, M.W. Wong, J.L. Andres, C. Gonzalez, M. Head-Gordon, E.S. Replogle, J.A. Pople, GAUSSIAN 98, Revision A.11.2, Gaussian Inc., Pittsburgh PA (1998).
30. W.L. Jorgensen, J. Phys. Chem. **90**, 1276 (1986).
31. W.L. Jorgensen, D.S. Maxwell, J. Tirado-Rives, J. Phys. Chem. **90**, 1276 (1986).
32. C.M. Breneman, K.B. Wiberg, J. Comput. Chem. **1**, 361 (1990).
33. K. Coutinho, S. Canuto, DICE: A Monte Carlo Program for Molecular Liquid Simulation, University of São Paulo (2003).
34. M.P. Allen, D.J. Tildesley, *Computer Simulation of Liquids* (Clarendon Press, Oxford, 1987).
35. R.C. Wilhoit, B.J. Zwolinski, J. Phys. Chem. Ref. Data **2**, 427 (1973).

36. J. Ridley, M.C. Zerner, Theor. Chim. Acta **32**, 111 (1973).
37. M.C. Zerner, Zindo: a semi-empirical program package, University of Florida, Gainesville 32611 (1999).
38. M. Leopoldini, T. Marino, N. Russo, M. Toscano, J. Phys. Chem. A **108**, 4916 (2004).
39. A. Lugasi, J. Hóvári, K.V. Sági, L. Biró, Acta Biol. Szeged. **47**, 119 (2003).
40. M. Orozco, F.J. Luque, Chem. Rev. **100**, 4187 (2000).
41. W. Xie, J. Pu, A.D. Mackerell jr., J. Gao, J. Chem. Theory Comput. **3**, 1878 (2007).
42. S. Canuto, K. Coutinho, Int. J. Quantum Chem. **77**, 192 (2000).
43. P. Jedlovszky, L. Turi, J. Phys. Chem. B **101**, 5429 (1997).
44. D. Swiatla-Wojcik, Chem. Phys. **342**, 260 (2007).
45. T. Andrade-Filho, H.S. Martins, J. Del Nero, Theor. Chem. Acc. **121**, 147 (2008).
46. G.M.A. Junqueira, W.R. Rocha, W.B. De Almeida, H.F. Dos Santos, J. Mol. Struc. (Theochem.) **719**, 31 (2005).
47. P. Trouillas, P. Marsal, D. Siri, R. Lazzaroni, J. Duroc, Food Chem. **97**, 679 (2006).
48. K. Robards, P.D. Prenzler, G. Tucker, P. Swatsitang, W. Glover, Food Chem. **66**, 401 (1999).
49. J.P. Cornard, L. Dangleterre, C. Lapouge, J. Phys. Chem. A **109**, 10044 (2005).
50. S. Canuto, K. Coutinho, D. Trzesniak, Adv. Quantum Chem. **41**, 161 (2002).
51. R. Rivelino, B.J.C. Cabral, K. Coutinho, S. Canuto, Chem. Phys. Lett. **47**, 13 (2005).
52. C.M. Aguilar, W.B. de Almeida, W.R. Rocha, Chem. Phys. **353**, 66 (2008).
53. G.M.A. Junqueira, W.R. Rocha, W.B. De Almeida, H.F. Dos Santos, Phys. Chem. Chem. Phys. **5**, 437 (2003).